

## Compressive behavior of a Zn<sub>22</sub>Al<sub>2</sub>Cu cellular alloy with different densities, microstructures and cell shapes

J. A. Aragon-Lezama<sup>a</sup>, A. Garcia-Borquez<sup>b</sup> and G. Torres-Villaseñor<sup>c</sup>

<sup>a</sup>Área de Ciencia de Materiales, Departamento de Materiales, Universidad Autónoma Metropolitana-A, Av. San Pablo 180, Col. Reynosa Tamaulipas, 02200 México, CDMX, México.

<sup>b</sup>Ciencia de Materiales, Escuela Superior de Física y Matemáticas-Instituto Politécnico Nacional, Edif. 9, Unid. Prof. A. López Mateos, Col. Lindavista, 07738 México, CDMX, México.

<sup>c</sup>Departamento de Materiales Metálicos y Cerámicos, Instituto de Investigaciones en Materiales - Universidad Nacional Autónoma de México, Apartado Postal 70-360, México, CDMX, México.

Tel: (55) 5318-9475 Ext. 9475 Fax (55) 53823998

e-mail: alja@correo.azc.uam.mx

Received 31 October 2020; accepted 17 December 2020

Zn<sub>22</sub>Al<sub>2</sub>Cu cellular alloy was prepared with six different densities, two microstructures and two cell shapes to determine the effect of these factors on its compressive behavior. NaCl granules with sharp edges, as purchased and with smooth edges obtained by roughly polishing the purchased granules were used as spacers. The elaboration process of the alloy foam consisted of melting the alloy, immersing the granules in the liquid alloy, air-cooling and then dissolving the salt in boiling water. The matrix obtained with the materials had an as-cast microstructure, and a fine microstructure, which was achieved with a heat treatment applied prior to dissolving the NaCl granules. Samples were tested in compression at a  $10^{-3} \text{ s}^{-1}$  strain rate. The smooth shape of the cells caused that the as-cast microstructure in the matrix produces an elastic behavior, which is described by the equation derived by Ashby for the relative elastic modulus and the relative density of sponges. The same type of cell shape embedded in the fine microstructure produces an elastic behavior in compression that depends on the density, which is typical of very low-density foams, although much lower than those achieved in this study. Compressive behavior is chaotic when cells have sharp shape, regardless microstructure type. The alloy studied with 4 mm mean size cells has a compression behavior like a sponge or low-density foam, when its cell walls have smooth contours, and as-cast or fine microstructure, respectively.

**Keywords:** Zn<sub>22</sub>Al<sub>2</sub>Cu cellular alloy; semi-solid processing; microstructural characterization; scanning electron microscopy; compression.

Se preparó una aleación celular de Zn<sub>22</sub>Al<sub>2</sub>Cu con seis densidades diferentes, dos microestructuras y dos formas de células para determinar el efecto de estos factores en su comportamiento compresivo. Como espaciadores se utilizaron gránulos de NaCl con bordes afilados, tal como se adquirieron, y con bordes lisos obtenidos mediante el desbaste de los gránulos adquiridos. El proceso de elaboración de la aleación celular consistió en fundir la aleación, sumergir los gránulos en la aleación líquida, enfriar al aire y luego disolver la sal en agua hirviendo. La matriz obtenida con los materiales tenía una microestructura recién colada y una microestructura fina, que se logró con un tratamiento térmico aplicado antes de disolver los gránulos de NaCl. Muestras se probaron en compresión a una rapidez de deformación de  $10^{-3} \text{ s}^{-1}$ . La forma lisa de las células provocó que la microestructura colada en la matriz produjera un comportamiento elástico, que se describe mediante la ecuación derivada por Ashby para el módulo de elasticidad relativo y la densidad relativa de esponjas. El mismo tipo de forma de célula incrustada en la microestructura fina produce un comportamiento elástico en compresión que depende de la densidad, propia de las espumas de muy baja densidad, aunque muy inferiores a las conseguidas en este estudio. El comportamiento en compresión es caótico cuando las células tienen una forma aguda, independientemente del tipo de microestructura. La aleación estudiada con células de tamaño promedio de 4 mm tiene un comportamiento de compresión como una esponja o espuma de baja densidad, cuando sus paredes celulares tienen contornos lisos y una microestructura de colada o fina, respectivamente.

**Descriptores:** Aleación celular Zn<sub>22</sub>Al<sub>2</sub>Cu; procesamiento semisólido; caracterización de microestructuras; microscopía electrónica de barrido; compresión.

PACS: 81.05.Zx; 83.50.Uv; 81.70.Bt

DOI: <https://doi.org/10.31349/RevMexFis.67.516>

### 1. Introduction

Cellular metals are a matrix with many voids or cells and are called foams when their cells are not interconnected or sponges when they are connected, as established by Ashby and Medalist [1].

These materials have drawn the interest of researchers, and engineers because of their diverse properties that sup-

port their multifunctional potential, as documented in an important and complete handbook of cellular metals written by Degischer and Kriszt [2].

More specifically, a piece of a cellular metal can be used for filters, noise or vibration dampeners, heat exchangers, packaging of fragile objects, catalysis support and in structures because low weights and adequate mechanical strength

are achieved. In addition, the properties of cellular metals could be further modified if the metal is a two-phase alloy whose microstructure changes with heat treatment, which increases its possible applications.

The Zn22Al alloy foam was already elaborated using the melt foaming method and  $\text{CaCO}_3$  as blowing agent to determine its compressive properties [3] and dynamic compressive strength [4]. This foam was as well processed with titanium hydride ( $\text{TiH}_2$ ) as a blowing agent to find the effect of porosity on tensile and compressive deformation [5].

The Zn22Al foam was additionally produced with short  $\text{Al}_2\text{O}_3$  fibers [6] or SiC [7] as stabilizing agents and reinforcement to assess the effect of these ceramics on compressive properties or compressive properties and damping, respectively. Moreover, the Zn22Al alloy was made like composite foam to establish the effect of different SiC contents on its compressive properties [8].

Open cell Zn22Al foams [9] and Zn22Al-1Cu foams with different microstructures [10], gotten by applying heat treatments, were produced by using preforms of NaCl and the process of replication to subsequently obtain the behavior and absorption capacity of energy under compression.

A study about closed-cell Zn-22Al foams was made using the powder metallurgy process, and its mechanical strain rate sensitivity was determined [11]. Moreover, a new composite-syntactic foam with different volume fractions (6-50 vol. %) of fly ash micro balloons coated with Ni, as the space holder material, was elaborated by the stir casting (vortex). Then, the effect of the ash volume fraction on microstructure, properties of compression and sensitivity of strain rate were determined for this material [12].

In addition, solid borosilicate glass spheres-Zn22Al2Cu composites were already elaborated and analyzed under compression as a function of their density and type of microstructure in the alloy matrix [13]. This material behaved similarly to cellular metals, but with collapse stresses (122.4-230.9 MPa) and plateau stresses (70-210 MPa) greater than those of conventional cellular metals ( $\sim 8 - 16$  MPa) [14]. This study provides, additionally, a new and simple method with high potential for the development of metal matrix composite materials with cellular behavior.

There are several methods to produce cellular metals: Nakajima [15] described the elaboration, properties and uses of metals with directional pores and Banhart [16] revised the manufacturing routes for metallic foams. One of these processes is to use granules or preforms of NaCl, which are embedded in the metal matrix and subsequently dissolved to form the cells.

For example, Yu *et al.* [9] used this method to elaborate open-cell Zn22Al foams, which they after mechanically characterized. Casolco *et al.* [17] manufactured close-cell Zn foams, and they followed the evolution of these foams. He-fa *et al.* [18] as well produced Al foams, which they later mechanically characterized, and Jian-Ning *et al.* [19] made a study on preparation of Zn-Al eutectoid alloy foamed by the infiltration process with air pressure and employed NaCl.

NaCl granules used in all these studies were irregular or cubic in shape.

In this study, the Zn22Al2Cu cellular alloy was processed with six different densities; it was separately used granules with sharp and smoothed edges as spacers, and the as-cast and fine-grained microstructure in the matrix. It is desired to establish how these parameters affect the compressive behavior of this alloy foam, and if this behavior is similar to that shown by the most cellular materials, following simple equations derived from the more known mechanical models for cellular metals.

## 2. Experimental

### 2.1. Alloy processing

The Zn22Al2Cu alloy was produced at  $700^\circ\text{C}$  by conventional casting using Zn, Al and Cu ingots with 99.99%, 99.27% and 99.999% purity, respectively. Appropriate amounts of the elements were weighed in a Mettler H45 precision balance ( $10^{-4}$  g). A total quantity of approximately 5 kg of alloy was elaborated.

A graphite crucible and a muffle type oven were used for the casting. The density of this alloy was  $5.4 \text{ g cm}^{-3}$  and was obtained using the Archimedes method.

### 2.2. NaCl granules and smoothing their shape

The NaCl used was natural and in the form of granules with irregular shapes, hereinafter referred to as granules with sharp shapes, and varied sizes. Its physical characteristics are a Young's modulus of approximately 40 GPa, melting temperature of  $816^\circ\text{C}$  and density of  $2.16 \text{ g cm}^{-3}$ .

Portions of the granules were sieved to obtain enough granules with sharp shapes and an average size of 4 mm. Other portions of granules of 200 g each, with an average size greater than 4 mm, were smoothed separately in a rotary device, which was designed and built for such purpose, having a rotatory cylindrical container with a sandpaper number 80 placed on its internal sidewall and base.

It was used an angular velocity of 65 to 75  $\text{rev}\cdot\text{min}^{-1}$  for 2 hours in each operation to smooth NaCl grain shape. Smoothing the granules causes them to fit better together and fill the spaces. Subsequently, these grains were sieved to select those with an average size of 4 mm.

### 2.3. Preparation of cellular alloy with different density

The cellular alloy with different density was obtained by first preparing composite materials with the Zn22Al2Cu alloy and NaCl granules. Each composite was prepared with 800 g of alloy and with a different portion of the salt granules to obtain composites with different densities: several of these portions had granules with sharp shapes, and other amounts of NaCl were granules with smoothed shapes. The composites were afterwards put in boiling water to dissolve the salt.

Each composite was prepared by melting and keeping the 800 g of alloy at 700°C and separately preheating the granules at 400°C. Subsequently, the heated granules were added to the melted alloy, and finally, each suspension was air-cooled: the granules were pushed into the liquid metal with a piston to prevent them from floating for an appropriate amount of time (suspensions obtained were not stirred) until the semisolid metal viscosity was sufficient, because more and more metal solidified as the cooling went on in the air, so that the granules were trapped inside the metal.

Every composite material was cut into two equal parts. One of them was heat treated, as described in Sec. 2.5, to change the microstructure in its metallic matrix.

The pieces of composite with different microstructures were submerged separately in boiling water for 20 minutes to dissolve the salt and then dried with a cloth and warm air. Later, the densities of cellular alloy pieces obtained were determined.

#### 2.4. Density calculation

The densities of the cellular alloy obtained were determined by calculating the mass/volume ratio of samples with dimensions of  $3.0 \times 3.0 \times 6.0 \text{ cm}^3$ . They were obtained using a high-speed cutting wheel. The measurements of the dimensions were made within 0.001 cm precision. The mass of each sample was measured with a precision of 0.0001 g on a Mettler analytical balance.

It was obtained densities of 1.9592, 2.4592 and  $3.0339 \text{ g cm}^{-3}$  and 2.1063, 3.0549 and  $3.2600 \text{ g cm}^{-3}$  when the shape of the cells in the alloy matrix was sharp and smooth, respectively.

#### 2.5. Matrix microstructures

The first matrix microstructure, called the as-cast microstructure, was obtained during air-cooling in the last stage of elaboration of the composites. The other microstructure was induced by a heat treatment in which the composite with the as-cast microstructure were heated and maintained at 350°C for 45.5 hours and quenched afterwards in acetone cooled at a 0°C temperature.

To visualize and characterize the microstructure of the alloy foams, samples of each microstructure were polished with a diamond suspension to get a scrapes free sample surface, and then that surface was chemically treated in  $\text{C}_2\text{H}_6\text{O}$  with 1% of  $\text{HNO}_3$ . Microstructures were characterized with a Leica Cambridge scanning electron microscope. Several zones were photographed and compositional analysis by EDXS was made in different microstructural constituents.

#### 2.6. Compression testing

Compression test and parameters of the obtained curves were realized and extracted following the ISO 13314: 2011 standard.

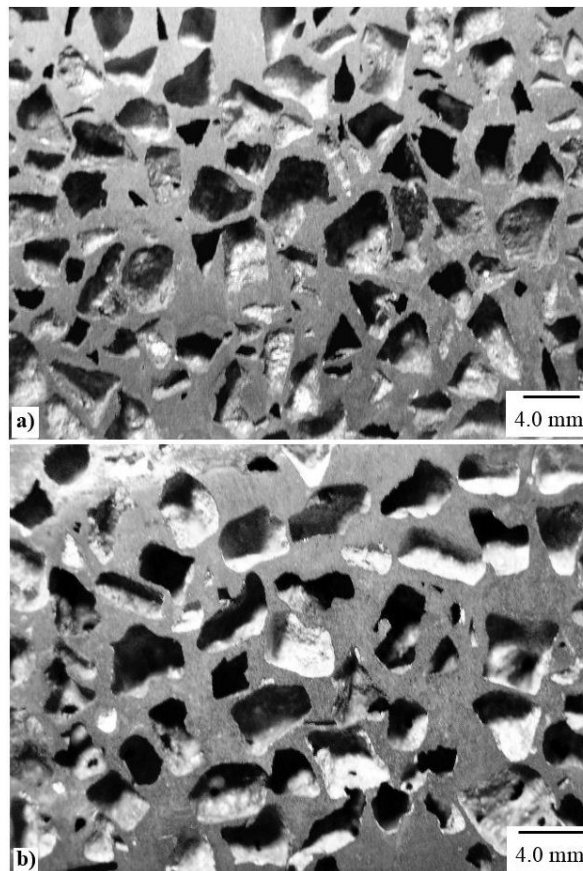


FIGURE 1. a) Section of the material with cells with sharp shapes and a density of  $2.4591 \text{ g cm}^{-3}$ . b) Section of the material with cells with smooth shapes and a density of  $3.2660 \text{ g cm}^{-3}$ .

Samples had dimensions of  $3.0 \times 3.0 \times 6.0 \text{ cm}^3$  and were tested under compression at a  $10^{-3} \text{ s}^{-1}$  strain rate in an Instron testing machine.

All samples were photographed before (Fig. 1) and after compression with an Olympus digital camera.

### 3. Theory

The compressive curve characteristic of cellular materials is formed by three zones: a first zone, called the elastic zone, where stress fluctuates linearly with strain, which finishes in a stress peak (named yielding point or collapse stress). A second zone, where stress varies slightly around a central stress value, called plateau stress, and a last zone, where stress increases substantially as strain increment, which is associated with the consolidation of cellular metals [20]: it is recognized that level of this curve increases as density enhances.

Because the properties of a cellular metal are affected to a greater or lesser extent by the shape, size, quantity and distribution of its cells, the cells could be considered as a “structural component”, even though these are void spaces and, consequently, consider the cellular metal as a type of “composite material”. Then, the rule of mixtures given by Eq. (1), originally developed for composite, could be applied to cellular materials,

TABLE I. Absolute and relative densities, volume fraction and percentages of cells of the alloy foam with cells with both shape types, and densities of the matrix and cells.

Alloy foam with cells with									
Sharp shapes				Smooth shapes				Matrix	Cells
$\rho_{AF}$	$\rho_r = \rho_{AF}/\rho_m$	$X_{ce}$	% vol.	$\rho_{AF}$	$\rho_r = \rho_{AF}/\rho_m$	$X_{ce}$	% vol.	$\rho_m$	$\rho_{ce}$
1.9592	0.3628	0.6372	63.72	2.1063	0.3900	0.6100	61.00	5.4	0
2.4592	0.4554	0.5446	54.46	3.0549	0.5657	0.4343	43.43	5.4	0
3.0339	0.5618	0.4382	43.82	3.2600	0.6037	0.3963	39.63	5.4	0

$\rho \equiv$  density (absolute) in  $g\ cm^{-3}$ ; AF  $\equiv$  alloy foam;  $m \equiv$  matrix;  $X \equiv$  volume fraction;  $ce \equiv$  cells;  $r \equiv$  relative; vol.  $\equiv$  cell volume.

$$\rho_{cm} = \rho_{ce}X_{ce} + \rho_m X_m, \tag{1}$$

where  $\rho$  is the density,  $cm$  is the cellular metal,  $ce$  is the cells,  $m$  is the metallic matrix and  $X$  is the volume fraction.

But because there is not material inside the cells,  $\rho_{ce} = 0$  in Eq. (1). This results in:

$$\rho_{cm} : \rho_m X_m \Rightarrow X_m : \rho_{cm}/\rho_m. \tag{2}$$

Considering also that it is always true that  $X_m + X_{ce} = 1$ , for which we find  $X_m = 1 - X_{ce}$ , and then Eq. (2) results in:

$$X_{ce} : 1 - \rho_{cm}/\rho_m = 1 - \rho_r, \tag{3}$$

where  $\rho_r = \rho_{cm}/\rho_m$  is the relative density.

Additionally, Ashby and Medalist [1] report that the elastic modulus of cellular metals in relation to that of the matrix,  $E_{cm}/E_m$ , varies in direct relation with the relative density,  $\rho_{cm}/\rho_m$ , (4):

$$E_{cm}/E_m = C_1(\rho_{cm}/\rho_m)^a, \tag{4}$$

where  $C_1$  is a constant,  $a = 2$  if the cells are not isolated (sponges), and  $a = 3$  when the cells is isolated (foams).

Ashby and Medalist [1] also state that the collapse and plateau stresses of cellular metals, respect to the yielding stress of the matrix,  $\sigma_{ym}$ , vary with the relative density, in according to

$$\sigma_{collapse}/\sigma_{ym}, \quad \sigma_{plateau}/\sigma_{ym} = C_2(\rho_{cm}/\rho_m)^{3/2}, \tag{5}$$

where  $C_2$  is constant.

## 4. Results

The two images in Fig. 1 show that most of the cells were clearly isolated (closed) on the surfaces resulting from the cut. Therefore, the correct name of the materials could be foams. However, when the compression test samples were observed under a nearby light source, the light crossed from one side of the compression test samples to another opposite side because they had a set of interconnected internal and external cells. So cell structures of samples were a combination

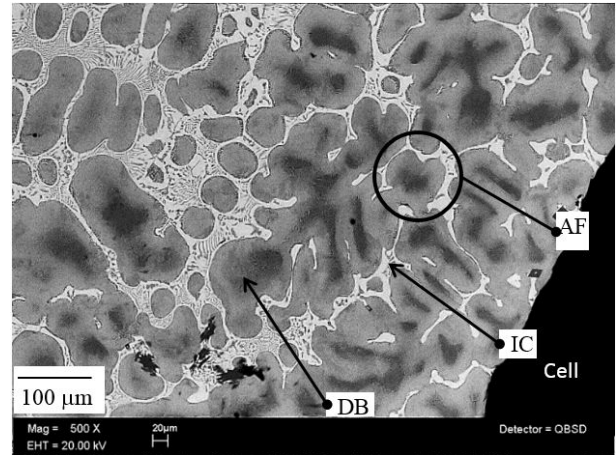


FIGURE 2. Representative area of the as-cast matrix microstructure of one half of the alloy foams elaborated. DB, dendritic branch; IC, inter-dendritic component, AF, area with fenced.

of open and close cells. Hereinafter the terms alloy foam or alloy foams will be used to refer to the material or materials studied.

### 4.1. Densities

Table I shows the absolute densities, relative densities, volume fraction and percentage of cells with both shape type obtained for the alloy foams; the table also shows the density assigned and obtained to the cells and the matrix, respectively. The volume fraction of cells was calculated using Eq. (3) in Sec. 3.

### 4.2. As-cast microstructure

Figure 2 shows a representative area of the casting matrix microstructure of one half of the alloy foams studied.

Figure 2 clearly shows the presence of dendritic branches, an inter-dendritic component and aspects that appear to be fenced areas with dark gray centers and light gray edges.

Dendrites and inter-dendritic component have a substructure of two components or alternating phases, one dark and one clear, that can be seen better at high magnifications, as in Fig. 3, which shows the dendritic substructure.

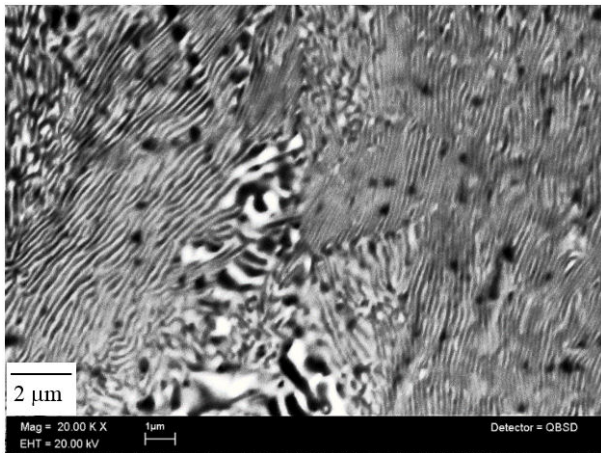


FIGURE 3. Substructure with alternating light and dark phases in the dendritic branches of casting microstructure of one half of the alloy foams studied.

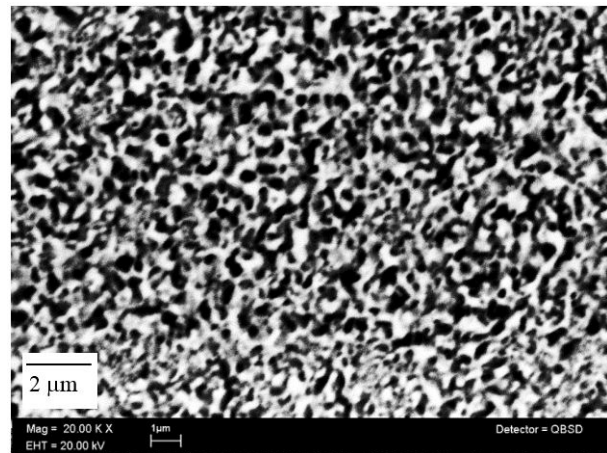


FIGURE 5. Fine substructure with two alternating phases, one rich in Zn with a light shade and the other rich in Al with a dark shade, in the matrix of the alloy foams with thermal treatment.

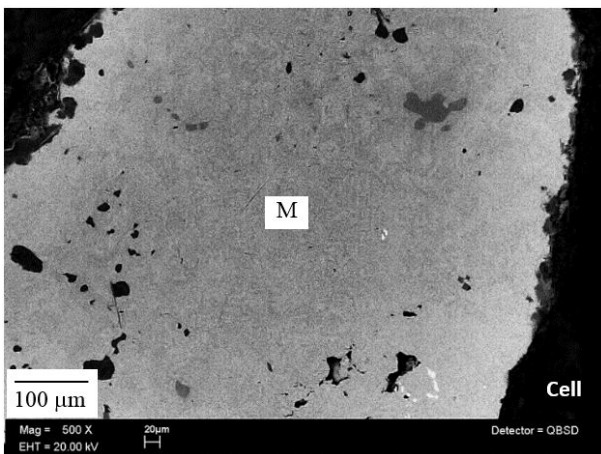


FIGURE 4. Representative area of the thermally induced microstructure in matrix, M, of one half of the alloy foams studied.

#### 4.3. Thermally induced microstructure

Figure 4 shows a representative zone of the thermally induced microstructure in matrix of one half of the alloy foams investigated.

At low magnifications, the matrices can be observed as large gray areas with some tiny black and light embedded islands. When the magnification is increased, a fine submicrostructure was observed, as shown in Fig. 5. The walls of the cells did not have cracks.

#### 4.4. Compression tests

Figures 6 and 7 show the curves of the nominal stress versus nominal strain of the alloy foam for the three densities achieved with cells with sharp and smooth shapes and with as-cast and fine-grained matrix microstructures, respectively.

## 5. Discussion

### 5.1. Densities

Table I clearly shows that the densities are in the lower range; therefore, the vol. % of cells is in the higher range when cells have sharp shapes.

### 5.2. As-cast microstructure

Compositional analysis by EDXS exposed that the dark centers of dendrites are Al rich; the two alternated bright and dark tonality constituents forming the inter-dendritic component and the substructure of dendrites are Al and Zn rich phases.

Fenced regions were formed in the casting microstructure because the peritectic transformation, at 72 wt.% Zn and 443°C, see Fig. 8, was incompletely verified due to non-equilibrium conditions existent during cooling of the last stage of the composites elaboration process. Al and Zn-rich alternated sheets are  $\alpha$  and  $\beta$  terminal phases, respectively.

These phases integrated the substructures of dendritic branches and the inter-dendritic component. The first substructure was formed via the eutectoid transformation, at 78 wt.% Zn and 275°C; the other substructure was created by an eutectic transformation at 95 wt.% Zn and 382°C (see Fig. 8).

### 5.3. Thermally induced microstructure

The fine-microstructure in the matrix was created by a beta-phase transformation that occurs in the Al-Zn system when eutectoid alloy is fast cooling from a temperature above 275°C. Sandoval-Jimenez *et al.* [22] report that a two stages transformation occurs: at the first stage, triclinic  $\beta$  phase, just after the alloy is fast cooled, transforms to a hcp  $\eta$  phase

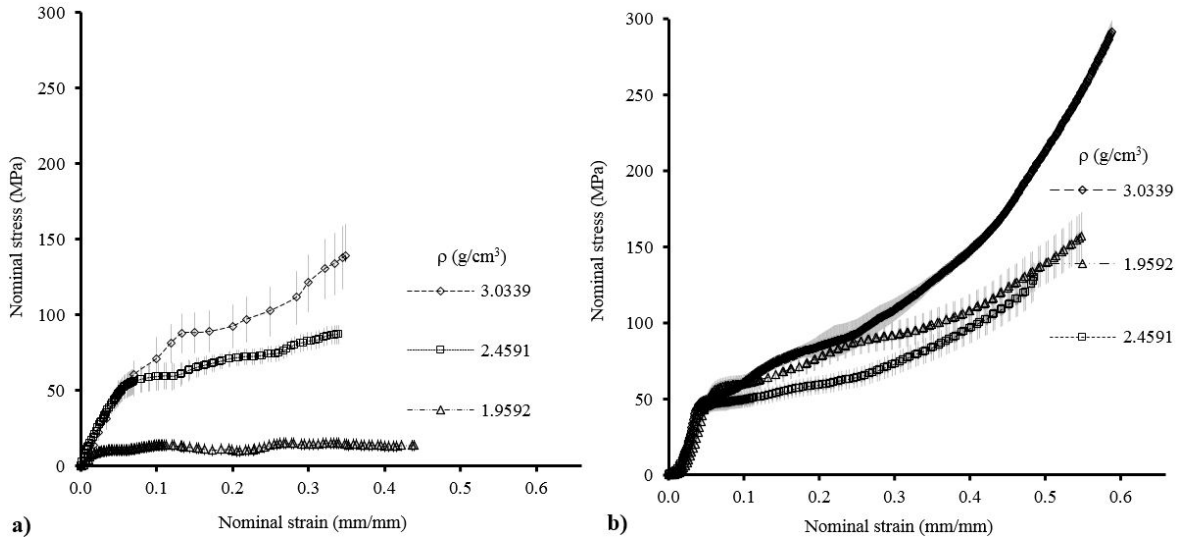


FIGURE 6. Nominal compressive stress as a function of nominal strain, for each density value and microstructure, a) as-cast and b) fine, of the matrix with sharp shapes cells.

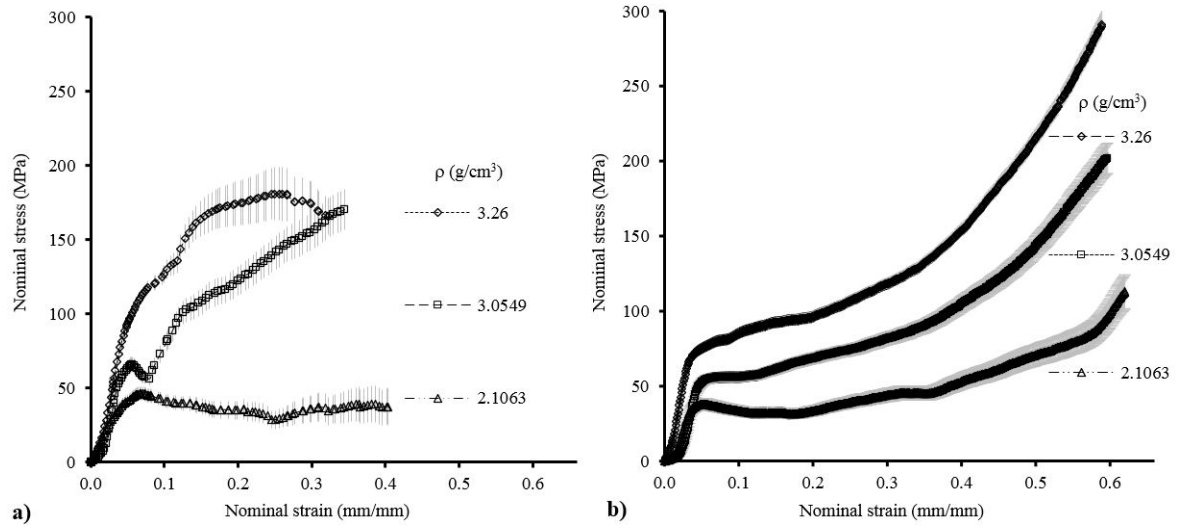


FIGURE 7. Nominal compressive stress as a function of nominal strain, for each density and microstructure, a) as-cast and b) fine, of the matrix with smooth shapes cells.

plus a second rhombohedral phase; the second stage: rhombohedral phase additionally changes to hcp  $\eta$  phase plus fcc  $\alpha$  phase.

Figure 9 shows an x-ray diffraction pattern of the matrix alloy with fine microstructure of foams studied:  $\alpha$  and  $\eta$  are equilibrium phases of the Zn-Al alloy system, see Fig. 8, and  $\varepsilon$  is an intermetallic phase with formula  $\text{CuZn}_4$ . This phase was not visualized in the image of the microstructure formed with the backscatter electron signal in the scanning electron microscope, because  $\varepsilon$  phase has a similar tone that  $\eta$  phase for being both phases abundant in elements (Cu and Zn or Zn, respectively) with a similar and high atomic weight. X-ray compositional mapping was not performed to locate  $\varepsilon$  phase because it was not an objective of this work.

Cell walls with fine microstructure were not cracked,

probably because the deformation of the NaCl granules used as the spacer material mitigated the contraction of the matrix when it solidified and during the quenching of the alloy-NaCl granules composite in the last stage of its preparation and of the heat treatment applied.

#### 5.4. Compression tests

The comparison of the compression curves obtained show that the alloy foam with smooth shapes cells, fine matrix microstructure and lowest density, as presented at the bottom of Fig. 7b, has the  $\sigma - \varepsilon$  graph that best shows all the features associated with the compression curves of cellular materials described at the beginning of Sec. 3.

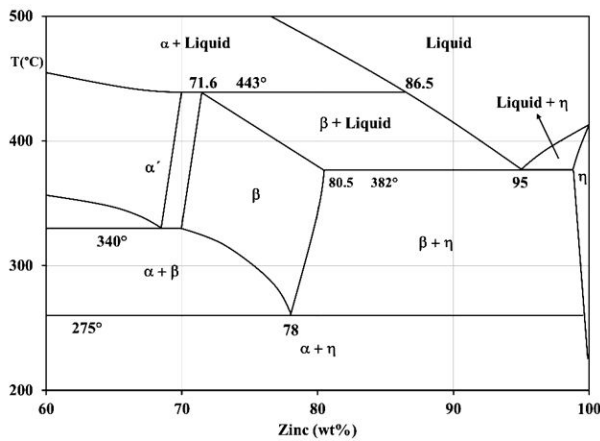


FIGURE 8. Side rich in Zn of the Al-Zn phase diagram deduced by Presnyakov *et al.*, [21].

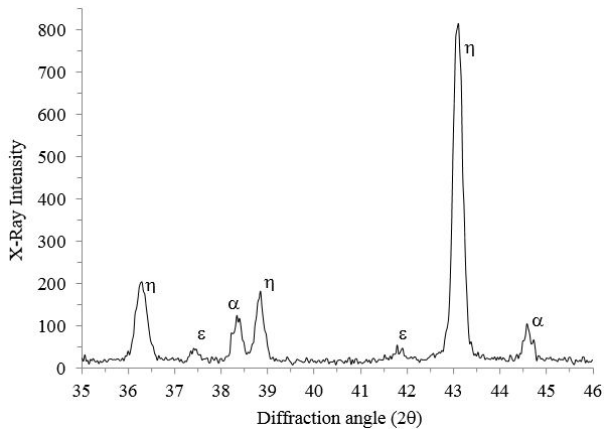


FIGURE 9. Diffraction pattern of the matrix alloy with fine microstructure.

More specifically, such curve has an initial zone of elastic deformation with linear variation between stress and strain, followed by a maximum or yield stress, called collapse stress. Next, there is a zone where the stress fluctuates slightly around a central value, which defines a type of plateau and, finally, a zone in which the stress continuously and substantially increases as strain increases, known as the consolidation region of the material.

As the density of the alloy foam with fine microstructure and cells with smooth shapes increases, the elastic modulus increases continuously and slightly (see Fig. 11a). The collapse stress tends to vanish: it is first observed as a maximum of stress and it transforms toward a point of inflection (see Fig. 7b), and its value increases progressively and slightly (see Fig. 11b). In addition, the density increase causes the plateau of stresses to occur at increasingly higher values and to decrease in extension until it almost disappears; it also causes the last densification region to start at increasingly higher stress values and lower strain values and the curve level increases substantially in these last two regions, as illustrated in Fig. 7b. This compression behavior becomes evident because the cells have a smoothed shape, and this is due

to diminishing of cells number when foam density increases.

If the fine microstructure is maintained and it has cells with sharp shapes instead of smooth shapes, the compressive behavior is chaotic and different from the above case (associated with cellular materials under compression and reported in the literature), as shown in Fig. 6b. Thus, the modulus of elasticity, shown in Fig. 10a, and collapse (or yield) stress shown in Fig. 10b, first decrease and then increase as density increases. No plateau can be seen in Fig. 6b, and the curve level does not increase as density does. The curves are very close for the two lowest density values; consequently, the last two regions of the curve of the alloy foam with higher density are slightly higher. Thus, it is believed that this compressive behavior is caused by the stress concentrations in the cell walls caused by the sharp edges of these same cells.

On the other hand, if the matrix microstructure is as-cast instead of fine and regardless of the shape of the cells, the compression curve of the lowest density alloy foam ends in a plateau and does not have a densification region, Figs. 6a and 7a. This is the case at least until an approximate strain value of  $\varepsilon = 0.4$ , at which point the test was stopped.

In contrast, with the alloys with fine microstructure and smooth cells, as their density increases, their densification starts approximately at  $\varepsilon = 0.20$ , 0.13 and 0.07. This means that the compressive behavior is different depending on the microstructure.

In addition, increasing the density of the alloy foam with the as-cast matrix microstructure causes a steady increase in the relative elastic modulus and relative collapse stress (see Figs. 11a and 11b) or an initial increase, and then, these two parameters remain constant, (see Figs. 10a and 10b), when the cells have sharp or smooth shapes, respectively.

At the same time, when the density increases, the plateau disappears, and the plastic zone level of the curves increases regardless of the shape of the cells, when alloy matrix has an as-cast microstructure, as shown in Figs. 6a and 7a. Then, it is evident that as-cast microstructure is less sensible to shape of cells than fine-grained microstructure is.

Florek [23] reports in his work on aluminum foams that certain characteristics of their compression curves indicate whether an aluminum foam has brittle or ductile behavior: a curve of a ductile aluminum foam has three characteristic zones (one of linear elasticity, another with a plateau and a final zone of consolidation), the first two zones are separated by an almost imperceptible collapse stress, followed by a plateau with a non-zero slope and a short extent (compared to a plateau in a compression curve of brittle aluminum foam) and the whole curve is smooth, without bulges (similar to the compression curve of cork [24]), whereas the curve of a brittle foam has a clear collapse stress, and if this stress is followed by a sharp drop a plateau may not be present on the curve, but if the compression curve has a plateau, it is extensive and has ripples. So, based on what is written here and in previous paragraphs, foams studied with fine microstructure have a behavior similar to that of ductile

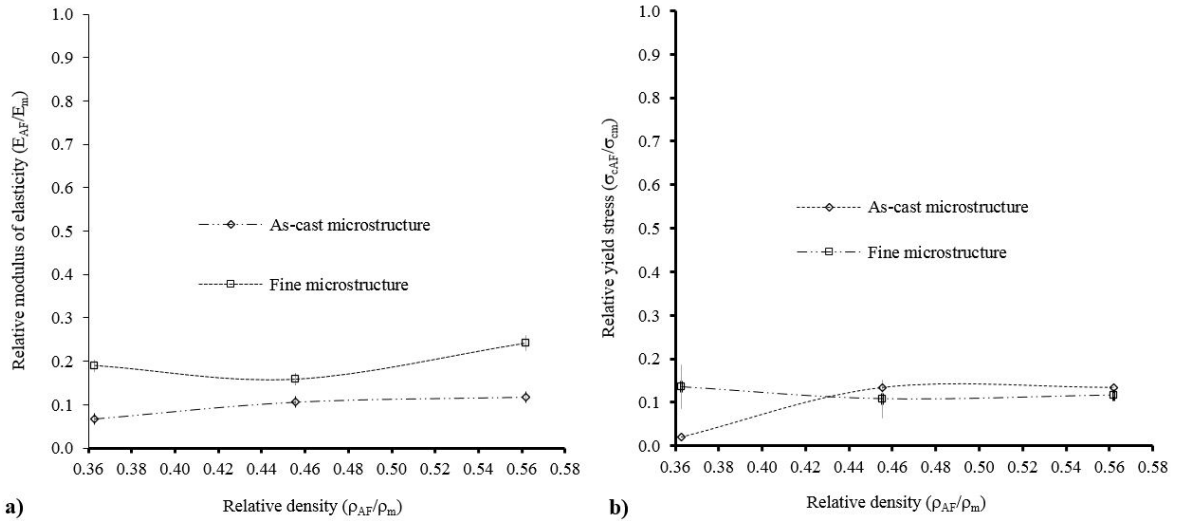


FIGURE 10. a) Relative modulus of elasticity and b) Relative yield (or collapse) stress versus the relative density of alloy foam with sharp edges cells and for as-cast and fine microstructures.

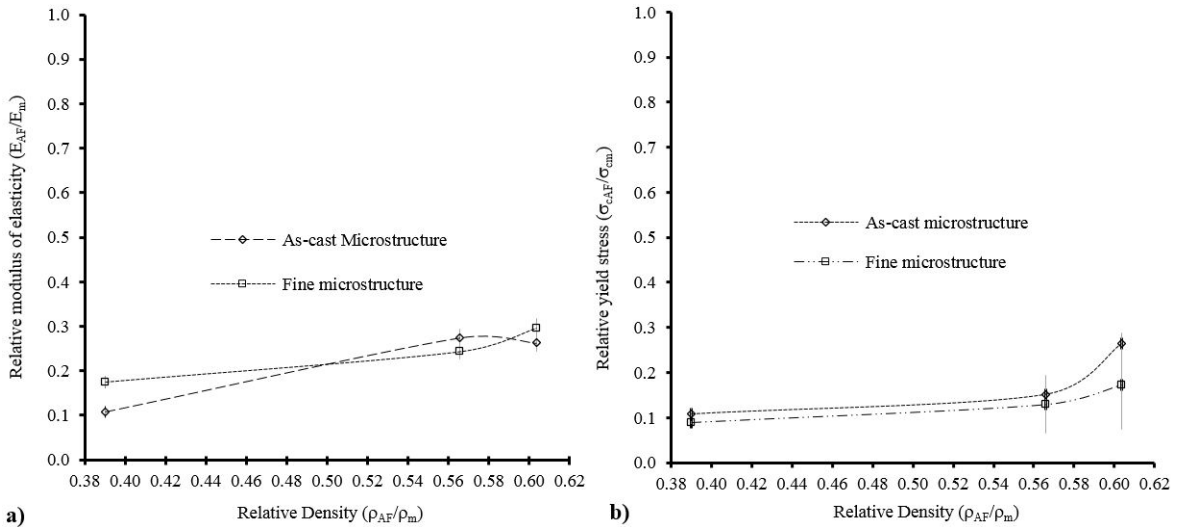


FIGURE 11. a) Relative modulus of elasticity and b) Relative yield (or collapse) stress versus the relative density of alloy foam with smooth shapes cells and for as-cast and fine microstructures.

aluminum foams, while the foams with casting microstructure behave like brittle aluminum foams.

In a previous work carried out by the authors of this work, using the same alloy matrix and microstructures but with embedded solid glass spheres [13], it was established in compression that the dendrites in as-casting microstructure are plastically deformed and micro-cracks are created, mainly in the inter-dendritic component. This makes the stress acting against the spheres is low when compression stresses are applied. While the tiny constituents of the fine microstructure are not deformed because they do not contain dislocations, as it was established by Torres *et al.* [25] when they exposed the properties and uses of the Zn22Al2Cu alloy, and, therefore, the stress is communicated almost directly from grain to grain and against the spheres. The authors of this work think that the same phenomena could be too happening when the

structural component is void spaces instead of glass spheres.

Then, it is possible that the stress concentrations produced by sharp edges, McClintock and Argon [26] prove that the holes or particles with sharp shape edges are the most severe stresses intensifiers, of cells were not attenuated because the local plastic deformation was null or too low at the tip of such cell edges, in the fine microstructure. Therefore, it is possible that sharp edges provoked the micro-cracks formation and fragility of alloy foam, Felbeck and Atkins [27] explain well about this in their book about strength and fracture of engineering solids, when the stress was applied. Therefore, it results a compression behavior more sensitive to cell shape change when the microstructure is fine.

At the end of the first paragraph of Sec. 3, it is written that the level of a compression curve increases in the order that foam density enhances. This variation pattern is observed



in graphs of Figs. 6a, 7a y 7b, but not in graph of Fig. 6b: because the curve of alloy foam with an intermediate density value has the lowest level. This anomalous behavior is due both to the response of fine microstructure of matrix and the effect caused by the sharp cell shape when compression stresses are applied.

The least squares method is used to establish how well the  $(\rho_{AF}/\rho_m, E_{AF}/E_m)$  data from the graphs in Figs. 10a and 11a fit model curves of type  $y = Cx^n$ , as defined by Eq. (4) in Sec. 3. Values of  $C = 0.2663$ ,  $n = 1.3187$  and  $R^2 = 0.8987$  (correlation coefficient) were obtained for the material with as-cast microstructure and cells with sharp shapes;  $C = 0.295$ ,  $n = 0.5304$  and  $R^2 = 0.2989$  were obtained for the material with fine microstructure and cells with sharp shapes.

Additionally, values of 0.8604, 2.1819 and 0.9674 were obtained for  $C$ ,  $n$  and  $R^2$ , respectively, for the material with as-cast microstructure and cells with smooth shapes;  $C = 0.4851$ ,  $n = 1.0911$  and  $R^2 = 0.9426$  were obtained for the material with the same cell shape (smooth) and fine microstructure.

In addition, the same fitting method was used on the data  $(\rho_{AF}/\rho_m, \sigma_{cAF}/\sigma_{cm})$  in the graphs in Figs. 10b and 11b to determine how well the data follow the relationship  $y = Cx^n$ , as defined by Eq. (5) in Sec. 3.

Values of  $C = 2.1111$ ,  $n = 4.2441$  and  $R^2 = 0.7695$  were calculated for the material with as-cast microstructure and cells with sharp shapes; for the material with the same cell shape and fine microstructure, the values established were:  $C = 0.09$ ,  $n = -0.358$  and  $R^2 = 0.4453$ .

Moreover, values of  $C = 0.50$ ,  $n = 1.6706$  and  $R^2 = 0.748$  were calculated for the material with as-cast microstructure and cells with smooth shapes;  $C = 0.3084$ ,  $n = 1.3365$  and  $R^2 = 0.9028$  were calculated for the material with the same cell shape and fine microstructure.

Thus, considering the correlation indexes ( $R^2$ ) obtained, the only alloy foam that satisfies the Ashby equation between the relative modulus of elasticity and relative density of sponges is that with as-cast microstructure and cells with smooth shapes, following the relationship:  $(E_{AF}/E_m) = 0.8684(\rho_{AF}/\rho_m)^{2.1819}$ , with  $R^2 = 0.9674$ .

In turn, the alloy foam with fine microstructure and cells with smooth shapes satisfies a near-linear dependence equation between the relative modulus of elasticity and relative density. This equation is similar to that deduced from the general model for these parameters of mechanical behavior under compressive stresses of foams when materials have very low densities, as deduced by Avallé *et al* [28], or relative densities lower than 0.1. More specifically, it satisfies the following equation:  $(E_{AF}/E_m) = 0.4851(\rho_{AF}/\rho_m)^{1.0911}$ , with  $R^2 = 0.9426$ . In addition, this material partially fulfills Eq. (5) in Sec. 3 proposed by Ashby for the relative plastic collapse stress and relative density of a cellular metal; it follows the equation:  $\sigma_{AF}/\sigma_{cm} = 0.3084(\rho/\rho_m)^{1.3365}$ , with  $R^2 = 0.9028$ .

The different functional relationship found between the relative elastic modulus and the relative density (quadratic type when the alloy matrix has a cast microstructure, and linear, when it is fine) if the cells embedded in the alloy has

TABLE II. Comparison of the data obtained for the alloy foam in this study and the information found for materials made from a Zn22Al alloy in other studies.

Matrix	Material	Matrix Microstructure	Energy absorption capacity (MJ/m <sup>-3</sup> )	Compressive strength (MPa)	Densities ratio ( $\rho_{AF}/\rho_M$ )	Process	Reference
Zn22Al2Cu	Alloy foam with cells with sharp shapes	As-cast	4.01 to 27.77 <sup>a</sup>	8 to 49*	0.3628 to 0.5618	Alloy melting, granule	This study
		Fine	17.87 to 24.12 <sup>a</sup>	42 to 53*			
Zn22Al2Cu	Alloy foam with cells with smooth shapes	As-cast	11.14 to 46.5 <sup>a</sup>	39 to 96*	0.39 to 0.604	immersion and air-cooling	
		Fine	11.06 to 29.74 <sup>a</sup>	35 to 67*			
Zn22Al	Composites-foams with SiC particles	As-cast	0.96 to 1.18 <sup>a</sup>	~ 3.5 to 4.64**	0.177 to 0.186	Stir-casting	[8]
Zn22Al with 1.0 Cu and 0.03 Mg	Open cell foams	As-cast	3 to 7.5 <sup>a</sup>	4.7 to 20***	0.279 to 0.396	Replication with NaCl preforms	[9]
Zn22Al	Composites of syntactic foam with fly ash micro balloons coated with Ni	Fined-grained	55 to 133 <sup>b</sup>	75 to 200**	0.623 to 0.962	Stir-casting	[12]

<sup>a</sup> $\epsilon = 0.34$ ; <sup>b</sup> $\epsilon = 0.60$  and strain rate of  $8.3 \times 10^{-4} \text{ s}^{-1}$ ; \*Yield or collapse stress, \*\*First maximum stress; \*\*\*Collapse stress;  $\rho$  is the density; AF is the alloy foam or syntactic foam.

smoothed shape, could be explained according to the participation degree of the cells in the matrix when compression is applied.

It is known that the fine microstructure is formed by dislocation free constituents [25] and therefore they do not deform, so the compressive stress is almost completely transmitted against the cells. This causes that cells determine more the elastic behavior of this microstructure, as it happens with foams have a very low density [29], because they have a large number of cells, and it is more common to find a linear relation between their relative elastic modulus and relative density.

Then, in summary, the smooth shape of the cells causes a more normal compressive behavior that allows the effect of changes in the matrix microstructure to be clearly distinguished. When alloy matrix has an as-cast microstructure, an elastic behavior is generated in compression as a function of density, similar to that of most sponges. This behavior follows an equation proposed by Ashby for sponges under compression stresses. The fine microstructure induces, in general, a compressive behavior with a higher elastic modulus than those obtained with the as-cast microstructure; this elastic behavior satisfies a linear equation between stress and strain like the foams with densities much lower than foams studied with fine microstructure matrix in this work.

In contrast, the compressive behavior of the Zn22Al2Cu alloy foam with cells with sharp shapes and regardless of its matrix microstructure does not follow any Ashby equations for cellular materials. This may be the result of both the sharp shape and the large size of the 4 mm cells. This partially matches with that reported for the Zn22Al alloy sponge [9] prepared using the replication process and 0.84-3.9 mm NaCl granules and tested in compression, because it is only reported that their relative collapse stress varies with the relative density as predicted by the Ashby model, given by Eq. (5) in Sec. 3.

Table II shows data obtained for the alloy foams analyzed in this study and for the materials made with the Zn22Al alloy in other studies. With this information, it can be inferred that in general, the alloy foams made in this study with as-cast or

fine microstructure have greater energy absorption capacity and higher compression strength values than Zn22Al foams with SiC particles or those with 1.0 Cu and 0.03 Mg. However, these parameters are lower than the same parameters founded for Zn22Al syntactic foam composites.

## 6. Conclusions

In general, the compression curves of the Zn22Al2Cu alloy foam having the lowest densities are typical of this type of material. The compression curves are at a higher level and/or are more separated from each other as the density increases if the cell shapes are smooth. This shape of the cells in as-cast microstructure in the matrix produces a behavior of elasticity in alloy foam during compression, which is described by the equation derived by Ashby for the relative modulus of elasticity and relative density of sponges. At the same time, that same type of shape in the cells embedded in fine microstructure creates an elastic behavior in compression as a function on density, which is typical of foams with very low relative densities, lower than 0.1, that is much lower than densities achieved in this work. Compressive behavior is chaotic and the effects of changing microstructure and density are difficult to identify when cell are sharp, regardless microstructure in matrix, being this more evident when matrix alloy has a fine microstructure. Foams with as cast or fine matrix microstructure have a compression behavior similar to fragile or ductile aluminum foams, respectively. The alloy studied with 4 mm mean size cells has a compression behavior like a sponge or low-density foam, when its cell walls have smooth contours, and as-cast or fine microstructure, respectively.

## Acknowledgments

We are grateful to Eliezer Hernández Mecinas, M.Sc. and Omar Novelo Peralta, Ph.D. of the Materials Research Institute of the National Autonomous University of Mexico for their invaluable work in the compression tests and support in the operation of the scanning electron microscope, respectively.

1. M. F. Ashby and R. F. Medalist, The mechanical properties of cellular solids, *Metall. Mater. Trans. A* **14** (1983) 1755, <https://doi.org/10.1007/BF02645546>.
2. H. P. Degischer and B. Kriszt, *Handbook of Cellular Metals: Production, Processing, Applications* (Wiley-VCH, New Jersey, 2002), pp. 181-182, <https://doi.org/10.1002/3527600558>.
3. J. Liu *et al.*, The compressive properties of closed-cell Zn-22Al foams, *Mater. Lett.* **62** (2008) 683, <https://doi.org/10.1016/j.matlet.2007.06.032>.
4. J. Liu *et al.*, Dynamic compressive strength of Zn-22Al foams, *J. Alloys Compd.* **476** (2009) 466, <https://doi.org/10.1016/j.jallcom.2008.09.007>.
5. K. Sekido and K. Kitazono, Effect of Porosity on Tensile and Compressive Deformations of Superplastic Zn-22Al Alloy Foam, *Mater. Sci. Forum* **735** (2012) 73, <https://doi.org/10.4028/www.scientific.net/MSF.735.73>.
6. J. Liu *et al.*, Effect of Al<sub>2</sub>O<sub>3</sub> short fiber on the compressive properties of Zn- 22Al foams, *Mater. Lett.* **62** (2008) 3636, <https://doi.org/10.1016/j.matlet.2008.04.013>.
7. S. Yu, J. Liu, Y. Luo, and Y. Liu, Compressive behavior and damping property of ZA22/SiC<sub>p</sub> composite foams, *Mater. Sci.*

- Eng. A* **457** (2007) 325, <https://doi.org/10.1016/j.msea.2006.12.089>.
8. : J. Liu *et al.*, Correlation between ceramics additions and compressive properties of Zn-22Al matrix composite foams, *J. Alloys Compd.* **476** (2009) 220, <https://doi.org/10.1016/j.jallcom.2008.09.069>.
  9. S. Yu *et al.*, Compressive property and energy absorption characteristic of open-cell ZA22 foams, *Mater. Des.* **30** (2009) 87, <https://doi.org/10.1016/j.matdes.2008.04.041>.
  10. S. R. Casolco, G. Dominguez, D. Sandoval, and J. E. Garay, Processing and mechanical behavior of Zn-Al-Cu porous alloys, *Mater. Sci. Eng. A* **471** (2007) 28, <https://doi.org/10.1016/j.msea.2007.03.009>.
  11. K. Kitazono and Y. Takiguchi, Strain rate sensitivity and energy absorption of Zn-22Al foams, *Scr. Mater.* **55** (2006) 501, <https://doi.org/10.1016/j.scriptamat.2006.06.001>.
  12. A. Daoud, Synthesis and characterization of novel ZnAl22 syntactic foam composites via casting, *Mater. Sci. Eng. A* **488** (2008) 281, <https://doi.org/10.1016/j.msea.2007.11.020>.
  13. J. A. Aragon-Lezama, A. Garcia-Borquez, and G. Torres-Villaseñor, Foam behavior of solid glass spheres-Zn22Al2Cu composites under compression stresses, *Mater. Sci. Eng. A* **638** (2015) 165, <https://doi.org/10.1016/j.msea.2015.04.048>.
  14. J. Banhart and J. Baumeister, Deformation characteristics of metal foams, *J. Mater. Sci.* **33** (1998) 1431, <https://doi.org/10.1023/A:1004383222228>.
  15. H. Nakajima, Fabrication, properties and application of porous metals with directional pores, *Prog. Mater. Sci.* **52** (2007) 1091, <https://doi.org/10.1016/j.pmatsci.2006.09.001>.
  16. J. Banhart, Manufacturing routes for metallic foams, *Solidif. Sci. JOM* **52** (2000) 22, <https://doi.org/10.1007/s11837-000-0062-8>.
  17. S. R. Casolco, A. Zanatta, A. Chavelas, and S. Valdez, Evolution of Zn+NaCl foams, characterization and interconnection in closed cell, *Supp. Proc. TMS* **3** (2009) 551.
  18. Ch. He-fa, H. Xiao-mei, W. Jian-ning, and H. Fu-sheng, Damping capacity and compressive characterization in some aluminum foams, *Trans. Nonferrous Met. Soc. China* **13** (2003) 1046.
  19. W. Jian-Ning, Ch. Zhang-Yong, and L. Gen-Mei, Study on preparation of foamed Zn-Al eutectoid alloy by air pressure infiltration process, *Asia-Pacific Eng. Technol. Conf.* **2017** (2017) 989, <https://doi.org/10.12783/dtetr/apetc2017/111113>.
  20. L. J. Gibson and M. F. Ashby, *Cellular Solids*, Ch. 5 (Pergamon Press, Oxford, 1988), pp. 196, <https://doi.org/10.1002/adv.1989.060090207>.
  21. A. A. Presnyakov, Y. A. Gotban, and V. V. Cherpyakova, Aluminum-Zinc Phase diagram, *Phys. Chem.* **55** (1961) 623.
  22. A. Sandoval-Jiménez, J. Negrete, and G. Torres-Villaseñor, Phase transformations in the Zn-Al eutectoid alloy after quenching from the high temperature triclinic beta phase, *Mater. Charact.* **61** (2010) 1286, <https://doi.org/10.1016/j.matchar.2010.07.014>.
  23. R. Florek, F. Simančák, M. Nosko, and J. Harnšková, Compression test evaluation method for aluminium foam parts of different alloys and densities, *Powder Metall. Prog.* **10** (2010) 207.
  24. M. Emília Rosa, An introduction to solid foams, *Philos. Mag. Lett.* **88** (2008) 637, <https://doi.org/10.1080/09500830802302014>.
  25. G. Torres-Villaseñor, J. Negrete, and L. Valdés, Propiedades y usos del Zinalco, *Rev. Mex. Fis.* **31** (1984) 489.
  26. F. A. McClintock and A. S. Argon, *Mechanical Behavior of Materials* (Addison-Wesley, Massachusetts, 1966), pp. 411-4123.
  27. D. K. Felbeck and A. G. Atkins, *Strength and fracture of engineering solids*, Ch. 14, 2nd ed. (Prentice Hall, New Jersey, 1996), pp. 308-326.
  28. M. Avalor, G. Belingardi, and A. Ibba, Mechanical models of cellular solids: Parameters identification from experimental tests, *Int. J. Impact Eng.* **34** (2007) 3, <https://doi.org/10.1016/j.ijimpeng.2006.06.012>.
  29. L. J. Gibson, Mechanical Behavior of Metallic Foams, *Annu. Rev. Mater. Sci.* **30** (2000) 191, <https://doi.org/10.1146/annurev.matsci.30.1.191>.